Arabian Journal of Chemistry (2023) **16**, 105115

King Saud University

Arabian Journal of Chemistry

www.ksu.edu.sa
www.sciencedirect.com

ORIGINAL ARTICLE

Protective effect of polysaccharide from the artificially cultivated *Sanghuangporus vaninii* against H_2O_2-induced toxicity *in vitro* and in zebrafish models

Zhang Zuofa [a,*], **Lv Guoying** [a,1], **Shen Meng** [b], **Song Tingting** [a], **Peng Juan** [a]

[a] *Institute of Horticulture, Zhejiang Academy of Agricultural Science, Hangzhou 310021, China*
[b] *Jiaxing Academy of Agricultural Science, Jiaxing 314000, China*

Received 7 April 2023; accepted 25 June 2023
Available online 29 June 2023

KEYWORDS

Sanghuangporus vaninii;
Purified polysaccharide;
Antioxidant activity;
Zebrafish;
L929 cells

Abstract PFSV-2 is a purified polysaccharide with good hypolipidemic activity from artificially cultivated *Sanghuangporus vaninii*. In this study, PFSV-2 was characterized by scanning electron microscopy, atomic force microscopy, X-ray diffraction, zeta potential, thermogravimetric analysis and the Congo red test. To assess the protective effect of PFSV-2, H_2O_2-induced oxidant injury on L929 cells and larval zebrafish models was employed. PFSV-2 significantly reduced H_2O_2-induced cytotoxicity in L929 cells by decreasing intracellular ROS levels and cell apoptosis. Furthermore, PFSV-2 had an obvious protective effect against H_2O_2-stimulated oxidative stress in larval zebrafish by decreasing heart rate and reducing ROS generation and cells death. Additionally, PFSV-2 decreased the production of MDA and increased the activity of antioxidant enzymes SOD and CAT in both L929 cells and larval zebrafish. These results suggested that PFSV-2 may be useful as an antioxidant in the medical and cosmetic industries.

1. Introduction

Reactive oxygen species (ROS) are attracting considerable attention due to their important role in the biological functions of organisms (Kim and Jiang, 2010). At low concentrations, ROS mainly act as intercellular signaling molecules and growth factors (Wang et al., 2016). However, excessive accumulation of ROS can have deleterious effects on biological macromolecules and induce the disorganization of cell structures (Barzilai and Yamamoto, 2004). Indeed, the fundamental pathogenic mechanisms of many diseases have been found to originate from oxidative damage (Poprac et al., 2017). Searching for antioxidants as functional foods or medicines has attracted considerable attention (Hui and Gao, 2022).

* Corresponding author.
E-mail address: zzf2050@163.com (Z. Zuofa).
[1] This author contributed equally to this work.
Peer review under responsibility of King Saud University.

Production and hosting by Elsevier

https://doi.org/10.1016/j.arabjc.2023.105115
1878-5352

In recent years, many natural antioxidants with no side effects have been employed to help protect the human body from oxidative damage. Epidemiological studies have revealed that intake of fresh vegetable, fruits, tea and wines (good source of natural antioxidants) is related to the reduction of the incidence of disease (Davovobasha et al., 2018). Dietary antioxidants include numerous phytochemicals such as vitamin A, vitamin C and vitamin E, α-tocopherol, β-carotene and phenolic compounds (Chandra et al., 2019). Mushrooms have been documented as a source of potentially safer natural antioxidants (Sánchez, 2017). Various antioxidant compounds such as polysaccharide, phenolic compounds, ascorbic acid, tocopherols and ergosterol have been isolated from mushrooms (Trznadel et al., 1990; Tsai et al., 2007).

The use of Sanghuangporus as a traditional medicine can be traced back 2000 years in China. As one of the most important species in Sanghuangporus, *Sanghuangporus vaninii* can be artificially cultivated, thus it occupies the largest share of the 'Sanghuang' application market (Zhou et al., 2022). A variety of active components including polysaccharides, terpenoids, flavonoids, polyphenols, etc., have been found in *S. vaninii* (Zhang et al., 2019). Polysaccharides, the major components of *S. vaninii*, have been the subject of several previous studies (Zhang et al., 2019).

Previously, our research group extracted and purified a novel polysaccharide (PFSV-2) with a molecular weight of 20.377 kDa from the fruiting body of *S. vaninii*; this was a heteropolysaccharide that was rich in fucose, galactose and mannose (Zhang et al., 2023). The backbone of PFSV-2 was composed of an → 6)-α-Gal*p* (1→, →2, 6)-β-Man*p*(1 → and → 2)-α-Fuc*p* (1 → and was branched at the O-2 position of the t-α-Man*p*(1→, the primary structure of PFSV-2 was exhibited in supplementary Fig. 1. It was found that PFSV-2 had outstanding lipid-lowering activity through decreasing lipid accumulation and levels of TC and TG in larval zebrafish. There is no doubt that the polysaccharides from *S. vaninii* are valuable for functional foods. However, the antioxidant activity of PFSV-2 has not been investigated. Accordingly, the present study investigated the antioxidant activity of PFSV-2 in L929 cells and zebrafish models.

2. Materials

2.1. Materials and reagents

PFSV-2 was extracted and purified from *S. vaninii* by our research group. Trypsin, H_2O_2, and the BCA protein test kit were obtained from Shanghai Baoman Biotech. Co., Ltd. Superoxide dismutase (SOD), catalse (CAT) and malondialdehyde (MDA) test kits were bought from the Nanjing Jiancheng Bioengineering Research Institute. L929 cells were obtained from China Infrastructure of Cell Line Resources (Beijing China). 3-(4, 5-dimethylthiazol-2-yl)-2, 5-diphenyl(MTT), acridine orange, 2,7- dichlorofluorescein diacetate (DCFH-DA) and dimethyl sulfoxide (DMSO) were purchased from Sigma (St. Louis, MO, USA).All other reagents were analytic reagents.

2.2. Characterization of PFSV-2

The surface morphology of PFSV-2 was observed by scanning electron microscopy (SEM, Philips XL 30 ESEM, Philips, Holland). The samples were fixed onto the sample stand and then sputter-coated with platinum powder for observation.

Atomic force microscopy (AFM, Multimode 8, Brooke Corporation, USA) of PFSV-2 was conducted according to the reported methods (Jin et al., 2006). Polysaccharide solution (1 μg/mL, 1 mL) was filtered through a 0.45 μm membrane and then dropped onto a mica sheet for AFM analysis. A Si_3N_4 probe was used to determine the micromorphological characteristic of PFSV-2.

X-ray diffraction (XRD) analysis of PFSV-2 was determined using an X-ray diffractometer (Siemens D 5000, Bruker, Germany). Patterns were recorded with a scanning speed of 1° /min and an incident current of 40 mA over a diffraction angle (2θ) range of 5–90.

A Zetasizer Nano S90 instrument (Malvern Instruments, UK) was used to determine the zeta potential of PFSV-2. Briefly, PFSV-2 was dissolved in distilled water (1 mg/mL) and analyzed in triplicate at 25 °C.

The thermal stability and mass loss of PFSV-2 during thermal treatment were monitored by differential scanning calorimetery (Discovery series DSC, TA Instruments, USA) and thermogravimetric analyzer (Discovery SDT 650, TA Instruments, USA). PFSV-2 powder (10 mg) was weighed and heated from 20 to 800 °C at a heat rate of 10 °C/min.

The conformation of PFSV-2 was determined by the Congo red test. Various concentrations of NaOH were added to a mixture of PSV (2 mg·mL^{-1}) and Congo red (80 μM) and the mixtures were left to stand for 10 min. The maximum absorption wavelength of the samples was recorded using a spectrophotometer (Shanghai Precision and Scientific Instrument Co., Ltd, Shanghai, China).

2.3. Investigation of the protection of PFSV-2 on L929 cells against H_2O_2-induced oxidative damage

2.3.1. Cell culture

L929 cells were cultured in a 5% CO_2 humidified atmosphere (37 °C). The cells were cultured using DMEM supplemented with fetal bovine serum (10%), of sodium pyruvate (110 μg/mL), streptomycin (100 μg/mL) and penicillin (100 unit/mL). The cells were incubated for 2 days and then seeded on a 96-well plate with a density of 1×10^4 cells/well.

2.3.2. Assessment of cell viability

After the medium was changed to serum-free medium for the L929 cells, different doses of PFSV-2 (100 and 200 μg/mL) and H_2O_2 (300 μM) were added to each well. After 24 h, the medium was removed and the cells were treated with MTT-containing medium (100 μg /mL) for 3 h.The medium was then aspirated and DMSO (100 μL) was added to the wells. The absorbance at 540 nm was recorded using a microplate reader (Model 680, Bio-Rad, USA).

2.3.3. Intracellular ROS generation

After the L929 cells medium was changed to the serum-free medium, the cells were pretreated with different concentrations of PFSV-2 (100 and 200 μg/mL) and incubated for 1 h. Then, H_2O_2 (300 μM) was added to the cells and allowed to incubate for 1 h. Then, the cells were treated with DCFH-DA solution (1.0 μg/mL). After 30 min, the fluorescence was measured with a microplate reader at 485 nm (excitation)/535 nm (emission).

2.3.4. Nuclear staining with propidium iodide (PI)

L929 cells were seeded on 24-well cell imaging plates with of 5×10^4 cells/well for 24 h. Then, the cells were pretreated with

PFSV-2 (100 and 200 μg/mL). After 24 h, the cells were treated with H_2O_2 (300 μM). After 30 min, cells were stained with PI (100 μg/mL, 1.0 mL) and incubated for 20 min at 37 °C. Finally, the cells were washed twice with PBS and observed by fluorescence microscopy (Nikon Instruments Co., Ltd, Tokyo, Japan) at 535 nm (excitation)/615 nm (emission).

2.3.5. Analysis of mitochondrial membrane potential (MMP)

Rh123, a cell-permeant cationic dye, was used to monitor the mitochondrial membrane. MMP depolarisation results in the loss of Rh123 from the mitochondria and a decrease in intracellular fluorescence (Satoh et al., 1997). After the cells were treated with PFSV-2 plus H_2O_2 as described above, Rh123 (10 μM) was added to the cell culture and allowed to incubate for 30 min at 37 °C. The cells were then washed twice with PBS and then observed by flow cytometry. The laser emission was at 480 nm, and a 530 nm long-pass filter was used (Shimizu et al., 1996).

2.3.6. Detection of apoptotic cells with acridine orange/ethidium bromide (AO/EB) staining

The AO/EB double staining method was used for the morphological assessment of apoptotic cells. L929 cells were seeded in 24-well microtiter plates (1×10^4 cells per well) for 24 h. The cells were pretreated with PFSV-2 for 3 h, then incubated with H_2O_2 (300 μM) for 3 h at 37 °C before dye solution (AO and EB 100 μg/mL, 4 μL) was added to each well. The cells were observed and photographed with a fluorescence light microscope.

2.3.7. Flow cytometric analysis of apoptotic cells

L929 cells were treated with PFSV-2 (100 or 200 μg/mL) for 3 h prior to exposure to H_2O_2 (300 μM). After 3 h, the cells were collected, washed and then resuspended in binding buffer (1×10^6 cells/mL). Then, annexin V-FITC (5 μL) and PI (5 μL) were added, and the cells were incubated for 15 min in the dark. Finally, the apoptotic cells were quantified and analyzed by flow cytometry.

2.3.8. Evaluation of MDA levels, and SOD and CAT activities of L929 cells

The L929 cells were pretreated with PFSV-2 (100 or 200 μg/mL) for 3 h and then exposed to H_2O_2 (300 μM). After 3 h, the L929 cells were harvested, washed and lysed with lysis buffer. The supernatant was utilised for the SOD, CAT and MDA analyses.

2.4. In vivo antioxidant activity against H_2O_2-induced oxidative stress in zebrafish model

2.4.1. Maintenance of zebrafish

This study was conducted in conformity with the guide for the Care and Use of Laboratory Animals. AB-type zebrafish were purchased from Suzhou Murui Biotech. Co. Ltd. The zebrafish were raised in a 3 L acrylic tank at 28.5 °C, with a 14/10 h light/dark cycle. Embryos were collected within 30 min after natural spawning.

2.4.2. Application of PFSV-2 and H_2O_2 to zebrafish embryos

Approximately 8 h post-fertilization (hpf), embryos were transferred to individual wells and maintained in embryo medium containing PFSV-2. After 1 h of incubation, the embryos were treated with H_2O_2 (5 mM) until 24 hpf. The surviving fish were then used for further experiments.

2.4.3. Measurement of heart rate, ROS generation and cell death in larval zebrafish

The zebrafish heart rates were measured according to the method of Kim et al. (2016). The zebrafish heart rates in all the groups were recorded at 2 days post-fertilization (dpf) under a microscope. Intracellular ROS generation and cell death were measured in live embryos using DCFH-DA staining and acridine orange according to the method of Kim et al. (2016). The zebrafish were observed and photographed under a fluorescence microscope. The Image J program was used to quantify the fluorescence intensity.

2.4.4. Evaluation of MDA levels, and SOD and CAT activity in larval zebrafish

The treated zebrafish larvae were used to prepare a homogenate with halogenation buffer (pH 7.8, 1 mL) at 4 °C. The homogenate was centrifuged (9000 rpm, 15 min) and then the supernatant was utilized for the SOD, CAT and MDA analyses.

2.5. Statistical analysis

All the results are expressed as mean ± standard deviation. Statistical analyses were performed using one-way analysis of variance (ANOVA). The statistical significance of differences between the groups was assessed using the Student's *t*-test and a level of $P < 0.05$ was considered to be statistically significant.

3. Results and discussion

3.1. Characteristics of PFSV-2

The surface morphology of PSFV-2 was determined by SEM, with the results shown in Fig. 1**a**. A relatively complete lamellar structure with some holes was observed, indicating the entanglement and aggregation of PFSV-2 induced by the polysaccharide chains and electrical charges (Wan et al., 2022).

AFM was used to determine the molecular morphology of PSFV-2with the results shown in Fig. 1**b**. The polysaccharide chain formed flame-like aggregates of uniform size and regularity. The height of PSFV-2 reached 24.5 nm, which was much higher than that of a single polysaccharide (0.1–1.0 nm) and suggested that the molecular aggregation of PFSV-2 was involved (Yang et al., 2022). The hydroxyl groups in the polysaccharide chains and hydrogen bond interactions caused

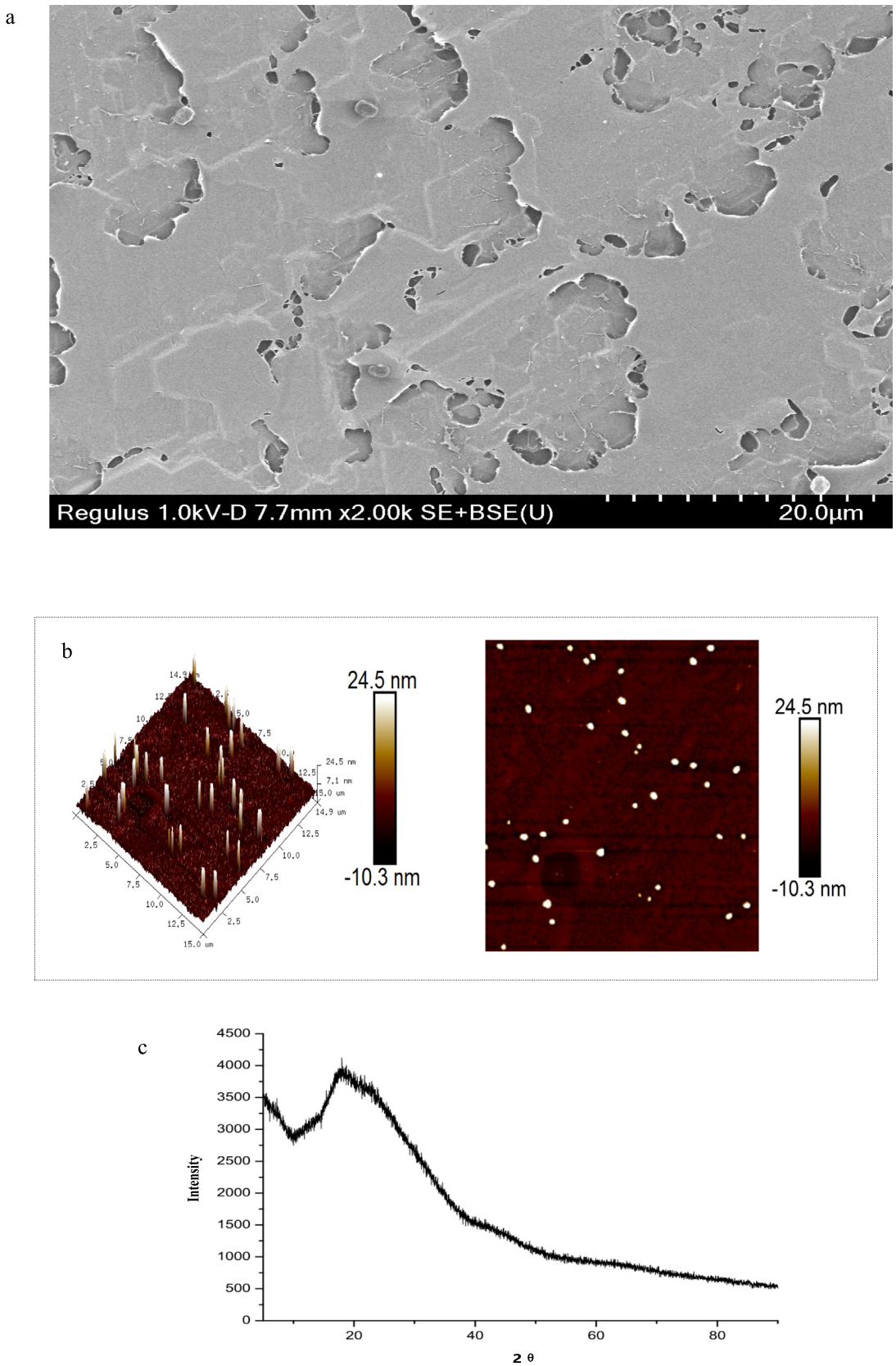

Fig. 1 Characterization of PFSV-2. (a) SEM, (b) AFM, (c) XRD pattern, (d) TGA trace, XRD pattern,(e) zeta potential, and (f) Maximum absorption wavelengths of Congo red and the Congo red/ PFSV-2 complex as functions of NaOH concentrations.

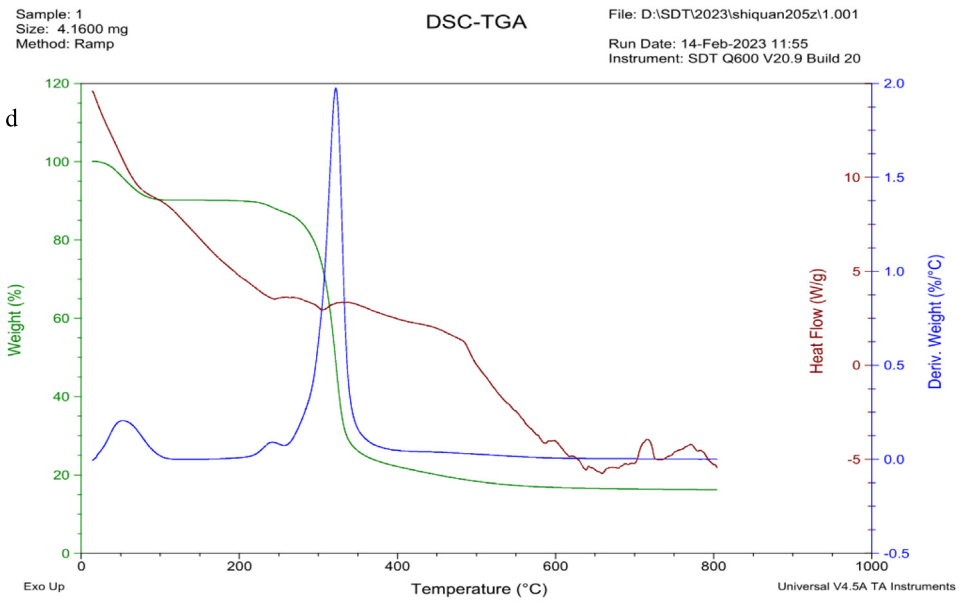

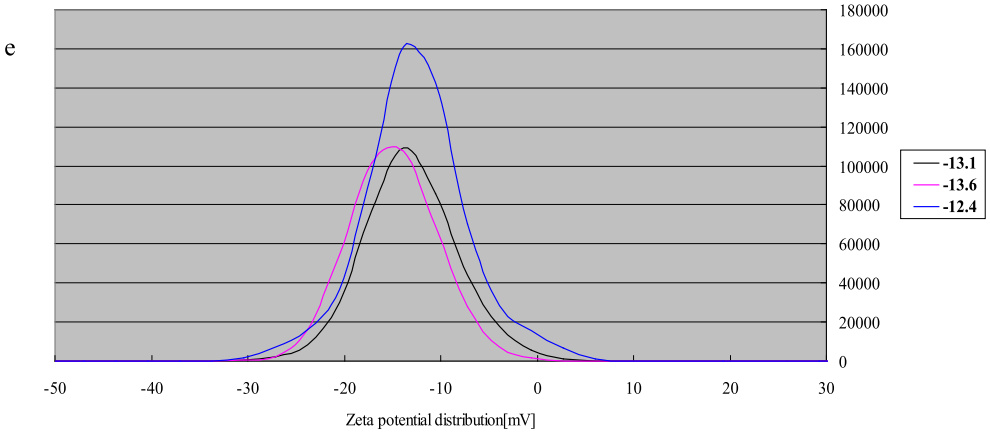

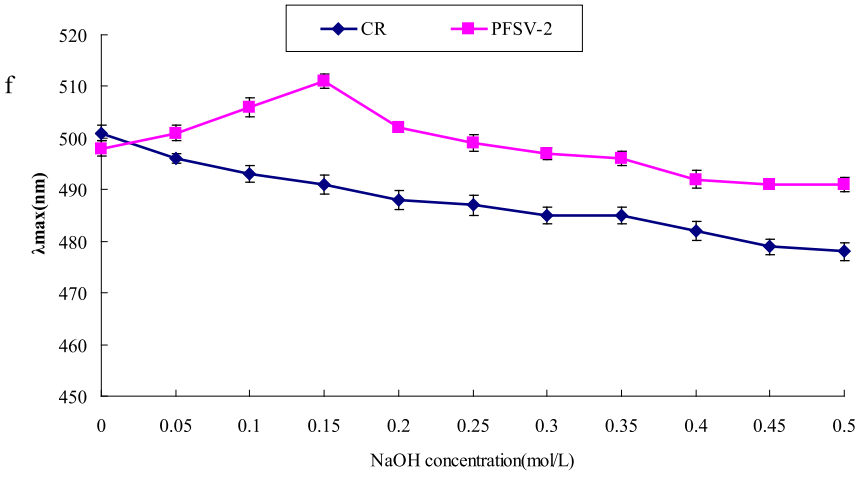

Fig. 1 (*continued*)

the chains to entangle with each other and form nonlinear ellipsoids or cylindrical structures (Henriksen et al., 2004).

XRD is a highly efficacious method for revealing the crystalline or amorphous nature of a polysaccharides. As shown in Fig. 1**c**, the XRD profile of PFSV-2 was characteristic, with one major reflection observed in the 5–90° 2θ region at 19.6°. This indicated that PFSV-2 contained one main crystalline component; hence, it was concluded that PFSV-2 was a semicrystalline polymer (Ren and Liu, 2020).

Stability is an important property when considering the biological applications of polysaccharides. In this study, the stability of PFSV-2 was examined by TGA. As shown in Fig. 1**d**, three main steps were involved in the decomposition of PFSV-2. In the first stage, 10% weight loss occurred below 220 °C, which was attributed to the loss of absorbed or hydrogen-bound water in the polysaccharide pores and the volatilization of a small amount of organic solvent (Archana et al., 2013). This indicated that PFSV-2 was stable at relatively low temperatures. The main weight-loss peak was observed at 250 °C, where the weight of PFSV-2 began decreasing sharply: approximately 70% of the initial weight was lost as the temperature was increased from 250 to 350 °C, which was mainly due to depolymerization reactions and the degradation of volatile components (Xie et al., 2013). During this stage, PFSV-2 underwent strong thermal cracking and its backbone began to break. Similar to the first stage, slow weight loss was observed during the third stage, during which the polysaccharide completely decomposed. Approximately 5% of the weight of PFSV-2 was lost during this stage (Ballesteros et al., 2015).

The charge of a polysaccharide can affect its stability, which directly determines its potential applications (Chen et al., 2021). As shown in Fig. 1**e**, the PFSV-2 solution had a charge of −13.03 mV, which indicated the strong electron-donating capacity and ease of coagulation of PFSV-2 (Li and Wang, 2016). For a polysaccharide, factors such as the charge density, physicochemical environment, molecular weight and type of wet-end additive are important factors that influence its zeta potential. The above results revealed the relative instability of the PFSV-2 solution (Wang et al., 2019a, 2019b). The polydispersity index (PDI) can reflect the distribution of individual molecular masses in a batch of polymers (Deng et al., 2021). According to our previous results, the PDI for PFSV-2 was 1.10, indicating that this polysaccharide had a narrow distribution of molecular weight without large aggregates (Zhang et al., 2023).

The conformation of the polysaccharide was analyzed by the Congo red test (Wang et al., 2019a, 2019b). Triple-helix polysaccharides react with Congo red, shifting to longer wavelengths at low concentrations and shorter wavelengths at higher concentrations of NaOH (Guo et al., 2018). As shown in Fig. 1**F**, the maximum absorption wavelength of PFSV-2 first increased and then decreased with increasing NaOH concentration. These results suggested that PFSV-2 had a triple-helix conformation.

3.2. Cell experiments

3.2.1. Influence of PFSV-2 on the survival rate of L929 cells

To evaluate the protective effect of PFSV-2 against H_2O_2-induced injury in L929 cells, the MTT assay was used to measure the viability of the L929 cells. As shown in Fig. 3**a,** the decreased cell viability induced by H_2O_2 (45.35 ± 3.87%) was significantly attenuated by PFSV-2 pretreatment in a concentration-dependent manner (100 μg/mL and 200 μg/mL PFSV-2remarkable increased cell viability to 67.28 ± 4.25% and 70.82 ± 3.62%, respectively). PFSV-2 These observations suggested that PFSV-2 protected L929 cells from H_2O_2-induced cell injury.

3.2.2. Effects of PFSV-2 on the ROS levels in L929

The DCFH-DA probe was used to evaluate the ROS levels in H_2O_2-treated L929 cells. As shown in Fig. 2**a, a** significant increase in DCF fluorescence was observed after H_2O_2 treatment, indicating high ROS levels ($p < 0.05$). The pretreatments of L929 cells with PFSV-2 (100 or 200 μg/mL) suppressed the increase in ROS in a dose-dependent manner (100 μg/mL and 200 μg/mL PFSV-2 inhibited intracellular ROS generation by up to 6.47 ± 0.67% and 4.28 ± 1.02%, respectively).

3.2.3. Protection of PFSV-2 against H_2O_2-induced nuclear damage in L929 cells

As shown in Fig. 2**b**, the red fluorescence of the H_2O_2-treated cells was significantly higher than that of the control groups. Pretreatment with PFSV-2 significantly reduced the red fluorescence (100 μg/mL and 200 μg/mL PFSV-2 reduced the nuclear damage to 38.16 ± 4.28% and 21.35 ± 3.16%, respectively). H_2O_2 treatment disrupted the cell membrane of L929, which resulted in more PI passing through the damaged cell membrane and improved the fluorescence intensity (Fan et al., 2022).

3.2.4. PFSV-2 prevented the loss of MMP in L929 cells

To assess the effect of PFSV-2 on the changes in MMP induced by H_2O_2 in L929 cells, flow cytometric analyses were carried out using Rh123. After the incubation of L929 cells with 300 μM H_2O_2 for 30 min, the MMP level was 16.72 ± 2.04% that of the control (Fig. 2**c**). Pretreatment with PFSV-2 protected cells against the H_2O_2-induced lowering of MMP: compared with the MMP in the control, the MMP level in cells incubated with 300 μM H_2O_2 was 31.50 ± 1.89% and 74.52 ± 4.42% in the presence of 100 and 200 μg/mL PFSV-2, respectively.

3.2.5. Effect of PFSV-2 on the nuclei of L929 cells

The morphological changes in L929 cells, as revealed by AO/EB staining, are shown in Fig. 2**d.** In the control group, the nucleus was arranged closely, chromatin was distributed uniformly and most of the cells emitted green light. After incubation with 300 μM H_2O_2, most of the L929 cells were in a state of apoptosis (orange and red, the ratio of dead cells reached 86.59 ± 3.86%). Pretreatment with PFSV-2 could reduce the apoptosis of cells in a dose-dependent manner (the ratios of dead cell reduced to 49.64 ± 4.18% and 11.41 ± 1.64% of 100 μg/mL and 200 μg/mL PFSV-2, respectively). This result indicated the PFSV-2 could diminish the ratio of apoptosis cells in L929 cells.

3.2.6. Effects of PFSV-2 on H_2O_2-induced apoptosis in L929 cells by flow cytometry

To verify the protective effect of PFSV-2 against H_2O_2-induced apoptosis in L929 cells, the annexin V-FITC/PI dou-

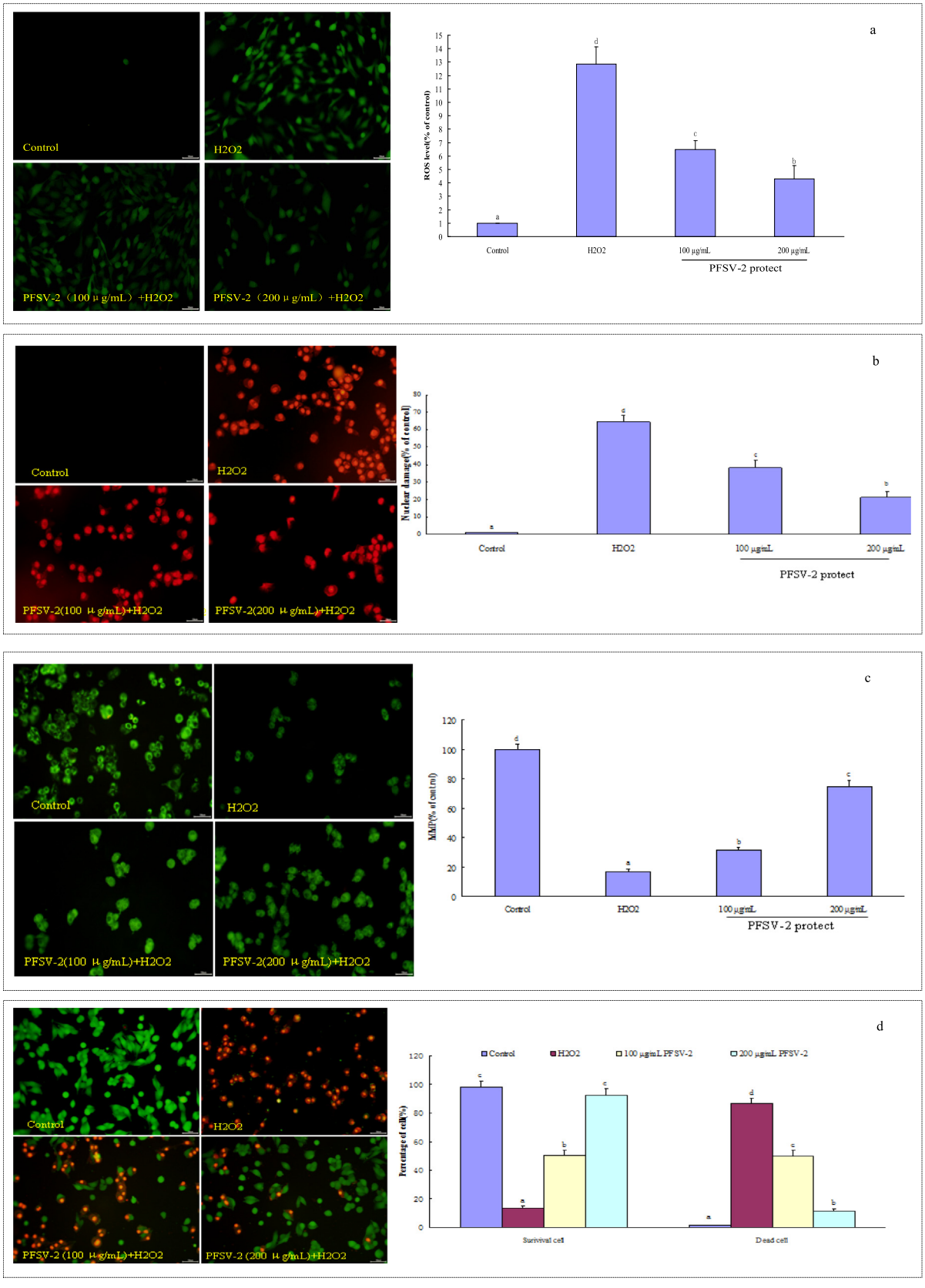

Fig. 2 PFSV-2 protects L929 cells against H2O2-induced oxidative damage. (a) ROS level using DCFH-DA staining, (b)nuclear damage using PI staining, (c) mitochondrial membrane potential detection using Rh123 staining, (d) morpholgical apoptotic cells using AO/EB staining, and (f) flow cytometric analysis of apoptotic cells using annexin V-FITC and PI staining.

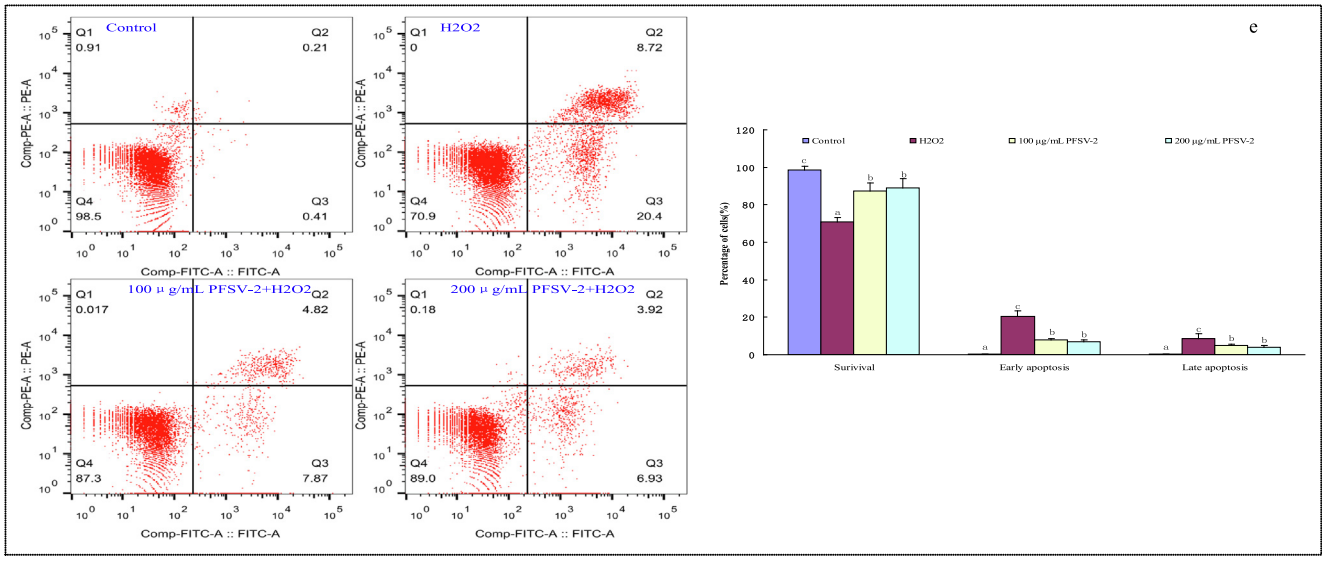

Fig. 2 (*continued*)

ble staining method was used to measure the cell apoptosis rates in different groups (Fig. 2**e**). In the scatter plot of flow cytometry, the Q_4 quadrant shows living cells; the Q_3 quadrant represents early apoptotic cells; the Q_2 quadrant stands for late apoptotic cells and the Q_1 quadrant acts for the dead cells. As displayed in Fig. 2**F**, the percentage of apoptotic cells was higher in the H_2O_2 group (20.41% early apoptosis and 8.72% late apoptosis) than that in the control group (0.41% early apoptosis and 0.21% late apoptosis). But a marked dose-dependent decrease in both the early and late stages of apoptosis occurred in the L929 cells after 100 and 200 μg/mL PFSV-2 treatments when compared with the H_2O_2 treated group.

3.2.7. Evaluation of MDA levels, and SOD and CAT activity

As shown in Fig. 3**b, c and d**, compared with the control group, H_2O_2 (300 μM) treatment could induced a significant decrease in the activity of SOD and CAT and an increase in the MDA levels in the L929 cells. However, the pretreatment of cells with PFSV-2 (100 and 200 μg/mL) distinctly ameliorated the decreased activity of SOD and CAT as well as markedly reducing the increased MDA levels induced by H_2O_2, in a concentration-dependent manner.

3.3. Protective effect of PFSV-2 against H_2O_2 in zebrafish

3.3.1. Influence of PFSV-2 on heart rate of zebrafish

The close relationship between oxidative stress and the heart rate of zebrafish has previously been reported (Kim et al., 2014). As shown in Fig. 4**a**, an elevation of the heart rate in zebrafish was observed after challenge with H_2O_2 when compared to the control. In contrast, pretreatment with different PFSV-2 concentrations significantly lowered the heart rate in a concentration-dependent mode. This result showed that PFSV-2 can alleviate H_2O_2-induced oxidative damage in the zebrafish model.

3.3.2. Effect of PFSV-2 on ROS production and cell death in zebrafish

DCFH-DA was used to measure the ROS production induced by H_2O_2 in zebrafish. As shown in Fig. 4**b**, the ROS levels in zebrafish treated with H_2O_2 increased significantly to 542.35 ± 31.96 % compared to the control group. In contrast, the zebrafish that were pretreated with different concentrations of PFSV-2 (100 and 200 μg/mL) had significantly decreased ROS levels of 312.42 ± 35.31 % and 283.57 ± 23.44 %, respectively. These results suggested the intracellular ROS abatement potential of PFSV-2 in zebrafish. Acridine orange, as a nucleic acid-selective fluorescent dye, was used to detect cell death in zebrafish. As shown in Fig. 4**c**, the cell death levels increased significantly to 286.36 ± 26.96% in the H_2O_2-treated group. However, in the presence of PFSV-2, the incidence of H_2O_2-induced cell death was significantly decreased.

3.3.3. Evaluation of MDA levels, and SOD and CAT activities in zebrafish

To further confirm the antioxidant effect of PFSV-2, the effects of H_2O_2 and PFSV-2 on the larval zebrafish were tested. As shown in Fig. 5.**a, b and c**, H_2O_2 reduced the activity of SOD and CAT, and PFSV-2 pretreatment resulted in the significant enhancement of SOD and CAT activity. Furthermore, compared with the control group, the H_2O_2-treated group showed significantly higher MDA levels and the PFSV-2 treatment exhibited a concentration-dependent decrease in MDA levels. All of the above results indicated that PFSV-2 could ameliorate the oxidative stress condition in zebrafish.

4. Discussion

As a type of ROS with non-free radical form, H_2O_2 can easily cross the cell membrane and injure the cell (Akhtar et al., 2017). Currently, H_2O_2 is used widely as an inducer of oxidative stress injury in the body (Fang et al., 2018). To explore

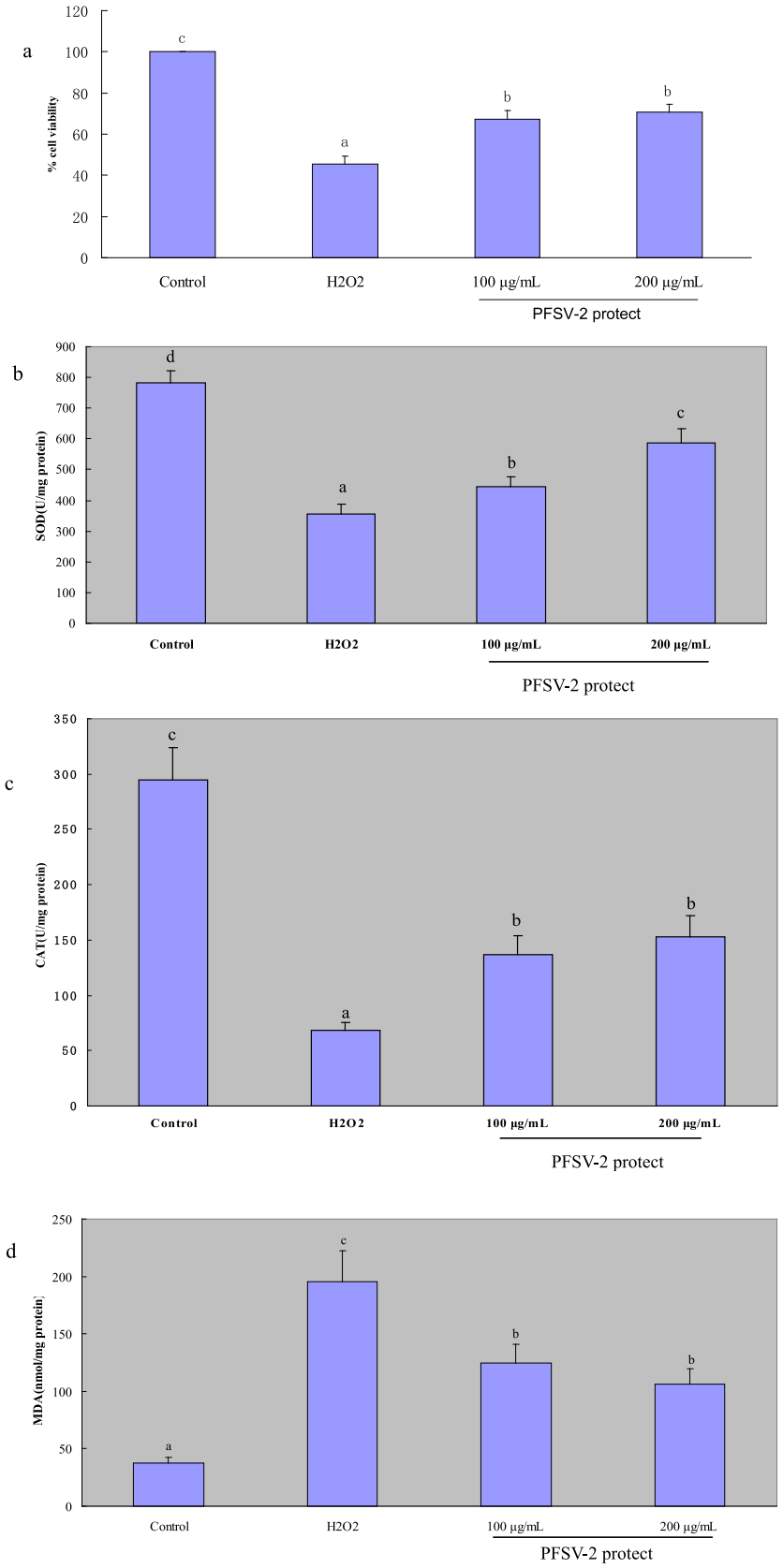

Fig. 3 (a) The protective effects of PFSV-2 against H_2O_2-induced cell death in L929 cells; (b)SOD activity of each treated cells; (c) CAT activity of each treated cells; (d) MDA content of each treated cells. Bar indicates means ± SD. Bars without the same superscripts (a-d) denote significant difference ($p < 0.05$).

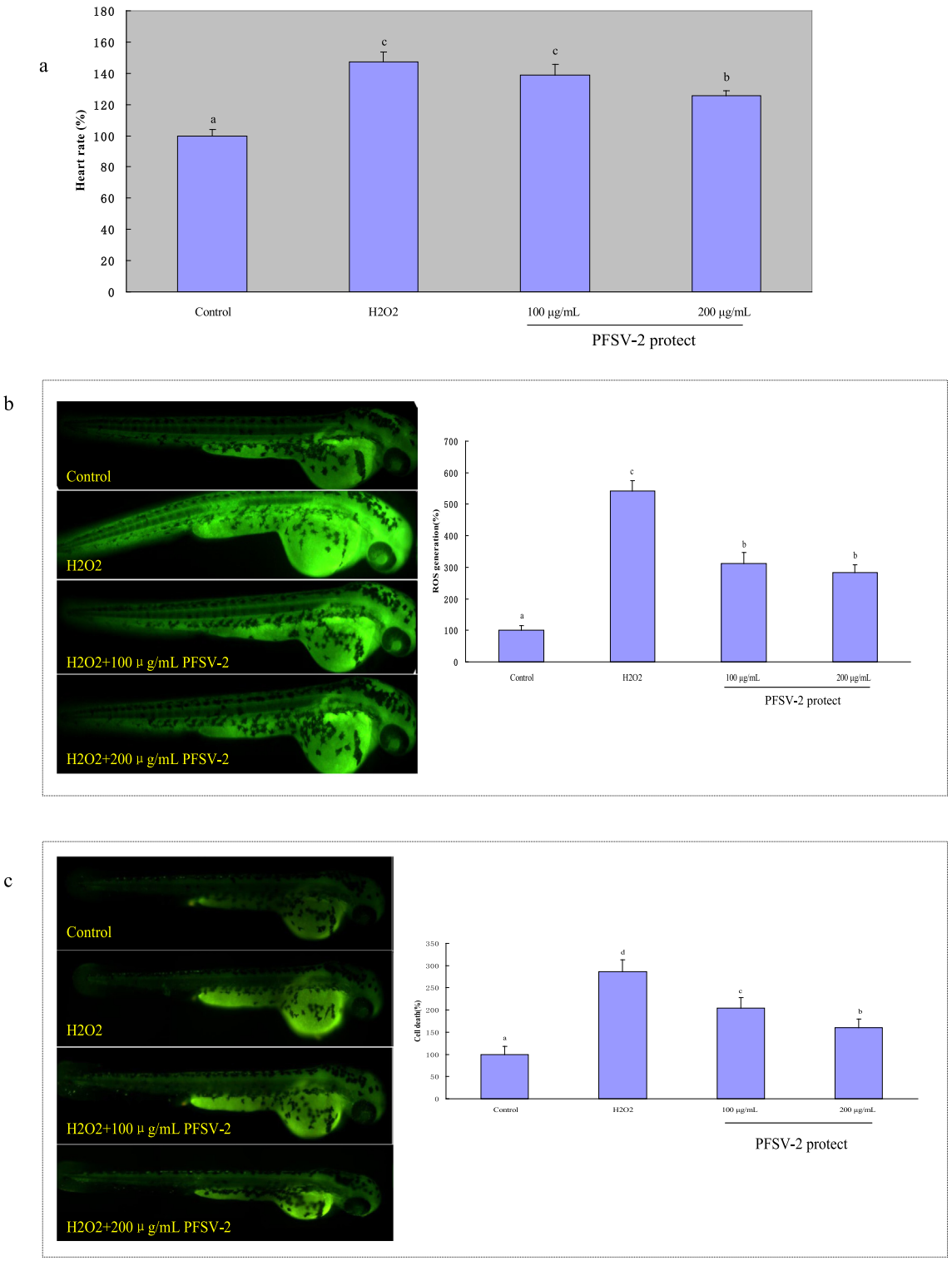

Fig. 4 The heart rates, ROS generation and cell death of zebrafish after pretreatment with PFSV-2 and/or treated with H_2O_2: (a) heart rate; (b) ROS generation, and (c) cell death. ROS and cell death levels were measured by Image J software. Bar indicates means ± SD. Bars without the same superscripts (a-d) denote significant difference ($p < 0.05$).

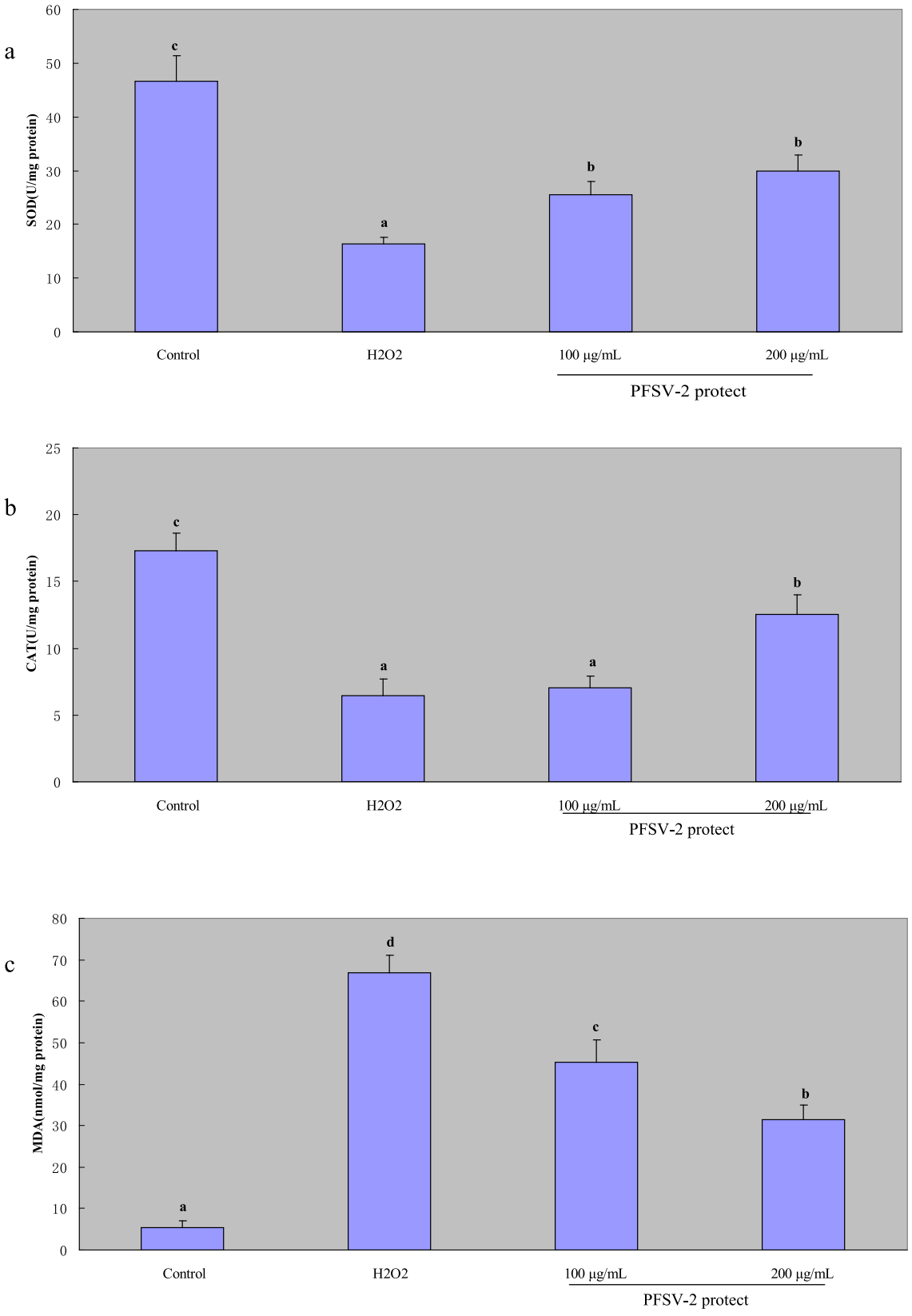

Fig. 5 The protective effects of PFSV-2 against H_2O_2-induced damage in zebrafish. (a) SOD activity of each treated zebrafish; (b) CAT activity of each treated zebrafish; and (c) MDA content of each treated zebrafish. Bar indicates means ± SD. Bars without the same superscripts (a-d) denote significant difference ($p < 0.05$).

whether PFSV-2 could protect cells and larval zebrafish from H_2O_2-induced oxidative damage, L929 cells and larval zebrafish were pretreated with PFSV-2 at two different concentrations and then treated with H_2O_2.

After exposure to H_2O_2, the survival rate of the cells that were pretreated with PFSV-2 was higher than that of the injury group, indicating that PFSV-2 exerted a protective effect on L929 cells against H_2O_2. In this study, H_2O_2 induced the rapid accumulation of ROS in L929 cells and larval zebrafish but PFSV-2 significantly decreased the ROS levels compared with the injury group. It is widely shared that excessive ROS generation can damage the mitochondrial membrane and result in cell death (Kroemer and Galluzzi, 2007). PFSV-2 could alleviate the damage induced by ROS by decreasing the aggravation of the MMP.

As an analogue of ethidium bromide, PI is a DNA staining reagent. PI can pass through the damaged cell membrane but not the intact living cell membrane (Kobayashi and Odake, 2017). Therefore, PI staining can be used to determine the integrity of the cell membrane. In the present study, the red fluorescence of the H_2O_2-treated groups was significantly higher than that of the control groups, indicating that H_2O_2 treatment disrupted the cell membrane. However, pretreatment with PFSV-2 significantly decreased the red fluorescence, indicating that PFSV-2 could alleviate the cell membrane damage induced by ROS.

AO/EB staining was used to distinguish between living and apoptotic cells (Xiang et al., 2020). Compared to the control, after L929 cell were exposed to H_2O_2, a higher percentage of apoptotic cells were detected. Pretreatment with PFSV-2 decreased the ratio of apoptotic L929 cells. This result indicated that PFSV-2 could protect the L929 cells against apoptosis.

Annexin V-FITC/PI labeling, followed by flow cytometry analysis, was used to confirm cell apoptosis. This assay could distinguish the viable cells, necrotic cells, and cells in early and late apoptosis. It was found that PFSV-2 pretreatment could decrease in both early- and late-stages apoptosis in L929 cells.

Over exposure to ROS can result in lipid peroxidation of the unsaturated fatty acids in the cell membrane (Amara et al., 2022). In this study, the MDA content was ascertained, which is the end product of lipid peroxidation and a biological marker of oxidative damage (Ferrer et al., 2009). PFSV-2 decreased the MDA levels in both cell and larval zebrafish models, exhibiting its protective effect. These results suggested that PFSV-2 could decrease the effects of oxidative stress and exhibit protective effects on L929 cells and larval zebrafish (Fig. 2**C,** Fig. 3**C**).

To further confirm the protective effect of PFSV-2 against oxidative stress, the activity of SOD and CAT (key antioxidant enzymes that scavenge ROS) following H_2O_2-induced oxidative injury in L929 cells and larval zebrafish models was assessed. The results showed that H_2O_2 treatment decreased the activity of SOD and CAT in both cells and larval zebrafish, while PFSV-2 could restore the activity of both enzymes in the H_2O_2-induced injury model *in vitro* and *in vivo*. Thus, PFSV-2 could restore the antioxidant system, which was a possible reason for the scavenging of ROS from injured cells and larval zebrafish. In a word, PFSV-2 could reduce the oxidative damage of H_2O_2 through scavenging intracellular ROS, protecting cell membrane, increasing the activities of antioxidant enzymes and reducing the cell apoptosis (Hu et al., 2022).

The antioxidant properties of polysaccharides are a result of the synergistic effects of various factors (Liu et al., 2021). Molecular weight, glycosidic bond type, monosaccharide composition and uronic acid content are the key factors that influence the antioxidant properties of polysaccharides (Ji et al., 2022). The antioxidant activity of polysaccharides is related to their electron- or hydrogen-donating capacity. Low molecular weight polysaccharides with good water solubility, higher surface areas and numerous exposed reducing ends have a higher chance of counteracting free radicals, granting them better antioxidant activity (Shang et al., 2021). Uronic acid can react with the hydrogen atom on the anomeric caribon, so the presence of uronic acid is considered to be another factor that is indicative of the antioxidant activity of polysaccharides (Wang et al., 2010).

The antioxidant activity of polysaccharides may be affected by the monosaccharide composition, which is due to the effects of the monosaccharide composition on the chain structure of polysaccharides (Chen et al., 2010). Lo et al. (2011) have reported that polysaccharides with a high proportion of mannose and rhamonse exhibited higher antioxidant activity. Additionally, polysaccharides with low glucose content are reported to have good antioxidant capacity (Chen et al., 2019). Recent studies have also found that polysaccharides with triple-helical structural integrity possess high antioxidant activity (He et al., 2016). Taking together, the strong antioxidant activity of PFSV-2 may be attributed to its low glucose content, low molecular weight and triple-helical structures. Further, research on the structure-effect relationship will inform the development of polysaccharide products with potential functional effects. Therefore, further studies are urgently needed to clarify the structure–activity relationship of PFSV-2.

5. Conclusion

The study indicated that the PFSV-2 purified from *S. vaninii* exhibited pronounced antioxidant activity *in vitro* and *in vivo*. PFSV-2 exhibited cytoprotective activity through increasing cell viability and the MMP, while decreasing ROS levels and L929 apoptosis. Additionally, PFSV-2 counteracted ROS generation and cell death and reduced the heart rate in the H_2O_2-induced oxidative stress *in vivo* zebrafish model. Furthermore, FPSV-2 decreased the production of MDA and increased the activity of antioxidant enzymes SOD and CAT in both the L929 cells and larval zebrafish. The above results open the possibility of exploitation of PFSV-2 as a novel therapeutic agent for oxidative stress diseases.

CRediT authorship contribution statement

Zhang Zuofa: Funding acquisition. **Lv Guoying:** Project administration, Investigation. **Shen Meng:** Project administration, Investigation. **Song Tingting:** Data curation. **Peng Juan:** Validation.

Declaration of Competing Interest

The authors declare that they have no known competing financial interests or personal relationships that could have appeared to influence the work reported in this paper.

Acknowledgements

The authors are grateful to Shanghai Sanshu Biotechnology Co., LTD for their help in characterization of PFSV-2. This research was funded by the New Variety Breeding Project of Science Technology Department of Zhejiang Province (2021C02073) and Agriculture, Rural areas and Farmers and nine-party Project of Zhejiang Province (2022SNJF047).

Appendix A. Supplementary material

Supplementary data to this article can be found online at https://doi.org/10.1016/j.arabjc.2023.105115.

References

Akhtar, M.J., Ahamed, M., Alhadlaq, H.A., Alshamsan, A., 2017. Mechanism of ROS scavenging and antioxidant signaling by redox metallic and fullerene nanomaterials: potential implications in ROS associated degenerative disorders. BBA-Gen. Subjects 1861, 802–813.

Amara, I., Timoumi, R., Annabi, E., Ben Othmene, Y., Abid-Essefi, S., 2022. The protective effects of thymol and carvacrol against di (2-ethylhexyl) phthalateinduced cytotoxicity in HEK-293 cells. J. Biochem. Mol. Toxicol. 36, e23092.

Archana, G., Sabina, K., Babuskin, S., Radhakrishnan, K., Fayidh, M.A., Babu, P., Sivarajan, M., Sukumar, M., 2013. Preparation and characterization of mucilage polysaccharide for biomedical for biomedical applications. Carbohyd. Polym. 98, 89–94.

Ballesteros, L.F., Cerqueira, M.A., Teixeira, J.A., Mussatto, S.I., 2015. Characterization of polysaccharides extracted from spent coffee grounds by alkali pretreatment. Carbohyd. Polym. 127, 347–354.

Barzilai, A., Yamamoto, K.I., 2004. DNA damage responses to oxidative stress. DNA repair 3, 1109–1115.

Chandra, P., Sharma, R.K., Arora, D., 2019. Antioxidant compounds from microbial sources: a review. Food Res. Int. 129, 108849.

Chen, H., Fang, C., Ran, C., Tan, Y., Yu, Q., Kan, J., 2019. Comparison of different extraction methods for polysaccharides from bamboo shoots (*Chimonobambusa quadrangularis*) processing by-products. Int. J. Biol. Macromol. 2019 (130), 903–914.

Chen, F., Miao, X., Lin, Z., Xiu, Y., Shi, L., Zhang, Q., Liang, D., Lin, S., He, B., 2021. Disruption of metabolic function and redox homeostasis as antibacterial mechanism of *Lindera glauca* fruit essential oli against *Shigella flexneri*. Food Control 130, 108282.

Chen, H., Xu, X., Zhu, Y., 2010. Optimization of hydroxyl radical scavenging activity of exo-polysaccharides from *Inonotus obliquus* in submerged fermentation using response surface methodology. J. Microbiol. Biotechnol. 20, 835–843.

Davoodbasha, M., Park, B.R., Rhee, W.J., Lee, S.Y., Kim, J.W., 2018. Antioxidant potentials of annoceria synthesized by solution plasma process and its biocompatibility study. Arch. Biochem. Biophys. 645, 42–49.

Deng, Q., Wang, W., Zhang, Q., Chen, J., Zhou, H., Meng, W., Li, J., 2021. Extraction optimization of polysaccharides from Gougunao tea and assessment of the antioxidant and hypoglycemic activities of its fractions *in vitro*. Bioact. Carbohyd. Dietary Fibre 26, 100287.

Fan, L., Wei, Y., Chen, Y., Jiang, S., Xu, F., Zhang, C., Wang, H., Shao, X., 2022. Epinecidin-1, a marine antifungal peptide, inhibits *Botrytis cinerea* and delays gray mold in postharvest peaches. Food Chem. 403, 134419.

Fang, S., Lin, F., Qu, D., Liang, X., Wang, L., 2018. Characterization of purified red cabbage anthocyanins: improvement in HPLC separation and protective effect against H_2O_2-induced oxidative stress in HepG2 cells. Molecules 24, 124.

Ferrer, E., Juan-García, A., Font, G., Ruiz, M.J., 2009. Reactive oxygen species induced by beauvericin, patulin and zearalenone in CHO-K1 cells. Toxicol. Vitro 23, 1504–1509.

Guo, Y., Cong, S., Zhao, J., Dong, Y., Li, T., Zhu, B., Song, S., Wen, C., 2018. The combination between cations and sulfated polysaccharide from abalong gonad (*Haliotis discus* hannai Ino). Carbohyd. Polym. 188, 54–59.

He, X., Niu, Y., Jin, M., Huang, J., Cui, H., Chang, Z., 2016. Characterization and antioxidation study of different weight of soluble soybean polysaccharides. Soybean Sci. 35, 805–809.

Henriksen, K., Stipp, S., Young, J.R., Marsh, M.E., 2004. Biological control on calcite crystallization: AFM investigation of coccolith polysaccharide function. Am. Mineral. 89, 1709–1716.

Hu, Y., Lu, S., Li, Y., Wang, H., Shi, Y., Zhang, L., Tu, Z., 2022. Protective effect of antioxidant peptides from grass carp scale gelatin on the H_2O_2-mediated oxidative injured HepG2 cells. Food Chem. 373, 131539.

Hui, H., Gao, W., 2022. Physicochemical features and antioxidant activity of polysaccharides from *Herba Patriniae* by gradient ethanol precipitation. Arab. J. Chem. 15, 103770.

Ji, X.L., Guo, J.H., Ding, D., Gao, J., Hao, L., Guo, X., Liu, Y., 2022. Structural characterization and antioxidant activity of a novel high-molecular-weight polysaccharide from *Ziziphus Jujuba* cv. Muzao. J. Food Meas. Charact. 16, 2191–2200.

Jin, Y., Zhang, H., Yin, Y., Nishiinari, K., 2006. Comparison of curdlan and its carboxymethylated derivative by means of rheology, DSC, and AFM. Carbohyd. Res. 341, 90–99.

Kim, G.N., Jiang, H.D., 2010. Protective mechanism of quercetin and rutin using glutathione metabolism on ho-induced oxidative stress in HepG2 cells. Ann. Ny. Acad. Sci. 1171, 530–537.

Kim, S.Y., Kim, E.A., Kim, Y.S., Yu, S.K., Choi, C., Lee, J.S., Kim, Y.T., Nah, J.W., Jeon, Y.J., 2016. Protective effects of polysaccharides from *Psidium guajava* leaves against oxidative stresses. Int. J. Biol. Macromol. 91, 804–811.

Kim, E.A., Lee, S.H., Ko, C.I., Cha, S.H., Kang, M.C., Kang, S.M., Ko, S., Lee, W., Ko, J., Lee, J., Kang, N., Oh, J., Ahn, G., Jee, Y., Jeon, Y., 2014. Protective effect of fucoidan aganist AAPH-induced oxidative stress in zebrafish model. Carbohyd. Polym. 102, 185–191.

Kobayashi, F., Odake, S., 2017. Intracellualr acidification and damage of cellular membrane of *Saccharomyces pastorianus* by low-pressure carbon dioxide microbubbles. Food Control 71, 365–370.

Kroemer, G., Galluzzi, L., 2007. Brenner, C. Mitochondrial membrane permeabilization in cell death. Physiol. Rev. 87, 99–163.

Li, X., Wang, L., 2016. Effect of extraction method on structure and antioxidant activity of Hohenbuehelia serotina polysaccharides. Int. J. Bio. Macromol. 83, 270–276.

Liu, H., Liu, X., Yan, Y., Gao, J., Qin, Z., Wang, X., 2021. Structural properties and antioxidant activities of polysaccharides isolated from sunflower meal after oil extraction. Arab. J. Chem. 14, 103420.

Lo, C.T., Cheng, A.C., Chiu, K.H., Tsay, P.K., Jen, J.F., 2011. Correlation evaluation of antioxidant properties on the monosaccharide components and glycosyl linkages of polysaccharide with different measuring methods. Carbohyd. Polym. 86, 320–327.

Poprac, P., Jomova, K., Simunkova, M., Kollar, V., Rhodes, C.J., Valko, M., 2017. Targeting free radicals in oxidative stress-related human diseases. Trends Pharmacol. Sci. 38, 592–607.

Ren, Y., Liu, S., 2020. Effects of separation and purification on structural characteristics of polysaccharide from quinoa (Chenopodium quinoa willd). Biochem. Biophys. Res. Commun. 522, 286–291.

Sánchez, C., 2017. Reactive oxygen species and antioxidant properties from mushrooms. Syn. Syst. Biotechno. 2, 13–22.

Satoh, T., Enokido, Y., Aoshima, H., Uchiyama, Y., 1997. Changes in mitochondrial membrane potential during oxidative stress-induced apoptosis in PC12 cells. J. Neurosci. Res. 50, 413–420.

Shang, H., Cao, Z., Zhang, H., Guo, Y., Zhao, J., Wu, H., 2021. Physicochemical characterization and *in vitro* biological activities of polysaccharides from alfalfa (*Medicago sativa* L.) as affected by different drying methods. Process Biochem. 103, 39–49.

Shimizu, S., Eguchi, Y., Kamiike, W., Waguri, S., Uchiyama, Y., Matsuda, H., Tsujimoto, Y., 1996. Bcl-2 blocks loss of mitochondrial membrane potential with ICE inhibitors acts at a different step during inhibition of death induced by respiratory chain inhibitors. Oncogene 12, 21–29.

Trznadel, K., Luciak, M., Pawlicki, L., Kedziora, J., Blaszczyk, J., Buczyinski, S., 1990. Superoxide anion generation and lipid peroxidation processes during hemodialysis with reused cuprophan dialyzers. Free Radic. Biol. Med. 8, 429–432.

Tsai, S.Y., Tsai, H.L., Mau, J.L., 2007. Antioxidant properties of *Agaricus balzei*, *Agrocybe cylindracea*, and *Boletus edulis*. LWT Food Sci. Technol. 40, 1392–1402.

Wan, C., Jiang, H., Tang, M., Zhou, S., Zhou, T., 2022. Purification, physico-chemical properties and antioxidant activity of polysaccharides from *Sargassum fusiforme* by hydrogen peroxide/ascorbic acid-assisted extraction. Int. J. Biol. Macromol. 223, 490–499.

Wang, B.H., Cao, J.J., Zhang, B., Chen, H.Q., 2019a. Structural characterization, physicochemical properties and α-glucosidase inhibitory activity of polysaccharide from the fruits of wax apple. Carbohyd. Polym. 211, 227–236.

Wang, L., Ding, L., Yu, Z., Zhang, T., Ma, S., Liu, J., 2016. Intracellular ROS scavenging and antioxidant enzyme regulating capacities of corn gluten meal-derived antioxidant peptides in HepG2 cells. Food Research Int. 90, 33–41.

Wang, J., Guo, H., Zhang, J., Wang, X., Zhao, B., Yao, J., Wang, Y., 2010. Sulfated modification, characterization and structure-antioxidant relationships of *Artemisia sphaerocephala* polysaccharides. Carbohyd. Polym. 81, 897–905.

Wang, D.Q., Wang, D.G., Yan, T.X., Jiang, W.F., Han, X.Y., Yan, J. F., 2019b. Nanostructures assembly and the property of polysaccharide extracted from *Tremella Fuciformis* fruiting body. Int. J. Bio. Macromol. 37, 751–760.

Xiang, L., He, B., Liu, Q., Hu, D., Liao, W.L.R., Peng, X., Wang, Q., Zhao, G., 2020. Antitumor effects of crucumin on the proliferation migration and apoptosis of human colorectal carcinoma HCT-116 cells. Oncol. Rep. 44, 1997–2008.

Xie, J.H., Liu, X., Shen, M.Y., Nie, S.P., Zhang, H., Li, C., Gong, D. M., Xie, M.Y., 2013. Purification, physicochemical characterisation and anticancer activity of a polysaccharde from *Cyclocarya paliurus* leaves. Food Chem. 136, 1453–1460.

Yang, B., Luo, Y., Sang, Y., Kan, J., 2022. Isolation, purification, structural characterization, and hypoglycemic activity assessment of polysaccharides from *Hovenia dulcis* (Guai Zao). Int. J. Biol. Macromol. 208, 1106–1115.

Zhang, Z., Lv, G., Cheng, J., Cai, W., Fan, L., Miao, L., 2019. Characterization and biological activities of polysaccharides from artificially cultivated *Phellinus baumii*. Int. J. Biol. Macromol. 129, 861–868.

Zhang, Z., Song, T., Chen, J., Lv, G., 2023. Recovery of a hypolipidemic polysaccharide from artificially cultivated *Sanghuangporus vaninii* with an effective method. Front. Nutr. 9, 1095556.

Zhou, L.W., Ghobad-Nejhad, M., Tian, X.M., Wang, Y.F., Wu, F., 2022. Current status of 'Sanghuang' as a group of medicinal mushrooms and their perspective in industry development. Food Rev. Int. 38, 589–607.